

# A Comparison On Cooling Curve Analysis Using Inc-Phatran And Winprobe

G. Sánchez Sarmiento<sup>1</sup>, Xiao (Leo) Chen<sup>2</sup>, Jorge Vega<sup>3</sup>, George Totten<sup>4</sup>, Ray Raynoldson<sup>5</sup>, Long Huynh<sup>5</sup> and Lemmy Meekisho<sup>6</sup>

1. Universidad de Buenos Aires, Facultad de Ingeniería. Buenos Aires, Argentina.
2. Automated Analysis Corporation, Peoria, IL, USA
3. SUDOSILO and Universidad Católica de Córdoba. Córdoba, Argentina.
4. Union Carbide Corporation, Tarrytown, NY, USA.
5. Quality Heat Treatment, Peoria, IL, USA.
6. Portland State University, Portland, OR, USA.

## Abstract

Cooling curve analysis was one of the principle methods for characterizing the heat transfer properties of the quenchant. Deriving the surface heat flux and heat transfer coefficient from a quenching probe test requires advanced inverse heat conduction algorithms. In this paper, the authors presented a comparison on the results of cooling curve analysis using both Inc-Phatran and WinProbe computer programs. The strengths and weaknesses of the programs were investigated through a few test cases.

## Introduction

Heat transfer coefficient is a critical parameter for both quenching practice and computer simulation of quenching processes. It may be used as a quantitative criterion for the comparison between different quenchant and it is a necessary boundary condition for modeling and simulating the quenching processes. As it is well known in this technological field, the overall quenching heat transfer mechanism may be complicated. For example, oil quenching exhibits at least three cooling phases: full-film boiling, nucleate boiling and convective cooling. Consequently it is difficult to direct model heat transfer between the quenchant and the part being quenched. Typically, heat transfer coefficients that are reported

## Algorithms in INC-PHATRAN

INC-PHATRAN Code<sup>3-8</sup> may be applied to simulate a great variety of heat treatment processes, in planar geometries as well as in axisymmetrical ones. The corresponding heat transfer coefficients can be calculated with its help, if cooling curves taken from different locations of the heat treated component are provided.

The model is based on a numerical optimization algorithm which includes a module responsible for calculating on time and space the temperature distribution and its coupled microstructural evolution.

The following unknown functions are determined in a coupled way:

- $T(\mathcal{P}, t)$ : Temperature.  $\mathcal{P} \in \Omega; t \in [0, t_f]$ ;
- $X_f(\mathcal{P}, t)$ : Volume fraction of austenite transformed to ferrite;
- $X_p(\mathcal{P}, t)$ : Volume fraction of austenite transformed to perlite;
- $X_M(\mathcal{P}, t)$ : Volume fraction of austenite transformed to martensite.

The heat conduction equation solved is:

$$\nabla \cdot (k(\mathcal{P}, T) \cdot \nabla T) + Q(T, \mathcal{P}, t) = c(\mathcal{P}, T) \rho(\mathcal{P}, t) \frac{\partial T}{\partial t} \quad (1)$$

$$\mathcal{P} \in \Omega; t \in [0, t_f]$$

are not associated with a specific cooling process and they are derived from experimental temperature-time data<sup>1</sup>.

The inverse heat conduction problem that consists in obtaining heat transfer coefficient based in measured cooling curves, is an ill-posed numerical problem of great complexity<sup>2</sup>. Present paper deals with a comparison between two different programs known in the literature that solves that numerical task: INC-PHATRAN and WinProbe. They are based on completely different numerical techniques. Cooling curves measured for Stainless Steel 304 quenched in helium and in oil are selected for this comparison.

At follows the algorithm of both codes are reviewed and the results of the numerical experiments are presented.

where  $k(\mathcal{P}, T)$ ,  $c(\mathcal{P}, T)$ ,  $\rho(\mathcal{P}, t)$  denote respectively the thermal conductivity, the specific heat and the density of the material.

$T(\mathcal{P}, t)$  is subjected to the initial condition:

$$T(\mathcal{P}, t = 0) = T_0(\mathcal{P}) \quad \mathcal{P} \in \Omega \quad (2)$$

and the boundary conditions:

$$-k \frac{\partial T}{\partial n} = q_i \quad \mathcal{P} \in \Gamma_i (i=1, \Lambda, m) \quad (3)$$

The term  $q_i$  may vary strongly along each partial boundary, adopting different expressions, depending on the heat transfer mechanism (convection, radiation) that governs the energy flow.

$Q(T, \mathcal{P}, t)$  represents the heat generation per unit volume and is split in two terms:

$$Q(T, \mathcal{P}, t) = Q_{PH}(T, \mathcal{P}, t) + Q_o(T, \mathcal{P}, t) \quad (4)$$

The first one accounts for the heat generation owing to microstructural transformations and takes the form:

$$Q_{PH}(T, \dot{V}, t) = \rho \left( H_F(T) \frac{dX_F}{dt} + H_P(T) \frac{dX_P}{dt} + H_M(T) \frac{dX_M}{dt} \right) \quad (5)$$

with:

- $H_F(T)$ : Heat of transformation from austenite to ferrite.
- $H_P(T)$ : Heat of transformation from austenite to perlite.
- $H_M(T)$ : Heat of transformation from austenite to martensite.
- $X_F(\dot{V}, t)$ : Volume fraction of austenite transformed to ferrite.
- $X_P(\dot{V}, t)$ : Volume fraction of austenite transformed to ferrite.
- $X_M(\dot{V}, t)$ : Volume fraction of austenite transformed to martensite.

The second term represents the contribution of other sources. When an induction heating process is considered,  $Q_o(T, \dot{V}, t)$  stands for the heat generation per unit time and per unit volume owing to eddy currents.

The transformation from austenite to ferrite, perlite and martensite phases is governed by isothermal transformation diagrams (TTT-diagrams) and the Avrami Time approach for the given material. The temporal evolution of each volume fractions may be represented by analytical expressions.

The solution of this set of equations is based on the finite element method for the discretization of the two-dimensional domain (cartesian and symmetry of revolution systems), and a Crank-Nicholson finite difference scheme for the time variable.

The temperature evolution, as measured by thermocouples at different positions in the component, are used as input for the program. The program calculates the time variation of the heat transfer coefficients, together with the temperature and distribution of phases, and their variation in time throughout the component.

In heat treating processes the energy is removed from the surface of the piece by convection and/or radiation. In some cases, the heat transfer coefficients are not known in advance and in others it is desired to optimize their values in order to make the treated piece undergo a prescribed thermal evolution. Provided that the temperature change inside the component and on its surface are measured, it is possible to solve the inverse heat transfer problem to determine the time variation of the heat transfer coefficients, that best satisfy productions demands.

Applying Newton's Law the boundary conditions are expressed by:

$$-k \frac{\partial T}{\partial n} = h_i (T - T_{am}) \quad \text{in } \Gamma_i \quad i = 1, \Lambda, p \quad (6)$$

where  $h_i(T)$  are the heat transfer coefficients corresponding to different portions of the boundary  $\Gamma$ , ( $\Gamma_1 \cup \Gamma_2 \cup \dots \cup \Gamma_p = \Gamma$ ;  $\Gamma_1 \cap \Gamma_2 \cap \dots \cap \Gamma_p = \emptyset$ ) and  $T_{am}$  the ambient temperature. Each one of these  $p$  cooling zones, has a time dependent heat transfer coefficient to be optimized. The time dependence of the heat transfer coefficient can be approximated by piece-wise linear functions or polygonal functions, each one defined by a set of parameters  $h_i^{(r)}$  ( $r = 1, \Lambda, p$ ;  $i = 1, \Lambda, q$ ), shown in figure 4.

The unknown design parameters can be expressed by the vector of  $m$  ( $m = p \times q$ ) components

$$\underline{\tau} = (\tau_1, \Lambda, \tau_m) = (h_1^{(1)}, \Lambda, h_q^{(1)}; h_1^{(2)}, \Lambda, h_q^{(2)}; \dots; h_1^{(p)}, \Lambda, h_q^{(p)})$$

The temperature at different instants of time may be measured by sensors at  $w$  points in the solid region, located at  $\bar{r}_k$ , ( $k = 1, \Lambda, w$ ). On calling  $T_k^m$ , the measured temperature, and  $T_k^c$ , the numerically calculated temperature at those points, one can pose the problem of obtaining the values of the heat transfer coefficients  $\tau_i$  that minimize the function:

$$S = S(\tau_1, \dots, \tau_m) = \sum_{k=1}^n (T_k^m - T_k^c)^2 = m \sum_{k=1}^n (T_k^m - T_k^c)^2 \quad (7)$$

being  $n$  the total number of measured temperatures, i.e. the number of points times the number of measurements at each point.

A necessary condition to satisfy (11) is that the following set of equations must be verified simultaneously:

$$F_i = \frac{\partial S}{\partial \tau_i} = -2 \sum_{k=1}^n (T_k^m - T_k^c) \frac{\partial T_k^c}{\partial \tau_i} = 0 \quad (i = 1, \Lambda, m) \quad (8)$$

A non-linear system of equations in the unknowns design parameters  $\tau_i$  is obtained by optimization algorithms.

### Algorithms in WinProbe

WinProbe is an in-house code for data post processing of quenching probe using one thermocouple at the center of the probe. A detailed discussion of the program functions and implementations can be found in references 1 and 9. WinProbe can compute the cooling rate, surface temperature, heat flux and heat transfer coefficient of the probe based on the cooling curve of the probe center. Cooling rate calculation was implemented using the Central Difference Scheme. Both lumped heat capacitance and inverse heat conduction models were implemented in WinProbe to calculate the heat flux and heat transfer coefficient.

The main computation algorithms in WinProbe are summarized as follows:

*Cooling Rate:*

$$\frac{\partial T}{\partial t} = \frac{Y^{n+1} - Y^{n-1}}{t^{n+1} - t^{n-1}} + O(\Delta t^2) \quad (9)$$

*Lumped Heat Capacitance Model:*

$$q = \frac{\rho \cdot C \cdot D}{4} \frac{\partial Y}{\partial t} \quad (10)$$

$$h = \frac{\rho \cdot C \cdot D}{4(T_\infty - Y)} \frac{\partial Y}{\partial t} \quad (11)$$

where  $Y$  is the measured temperature;  $\Delta t$  the time step;  $n$  the time step index;  $D$  the probe diameter;  $q$  the heat flux; and  $T_\infty$  the bulk or quenchant temperature.

Inverse Heat Conduction Model:

$$\frac{1}{r} \frac{\partial}{\partial r} \left( kr \frac{\partial T}{\partial r} \right) = \rho C \frac{\partial T}{\partial t} + \eta \frac{\partial^2 T}{\partial t^2} \quad (12)$$

$$T_{i+1} = T_i + \frac{2}{\alpha_i} \frac{r_i \Delta r^2 \frac{\partial T_i}{\partial t} + (T_i - T_{i-1})(r_i + r_{i-1})}{r_i + r_{i+1}} - \eta' \frac{\partial^2 T}{\partial t^2} \quad (13)$$

$$q^n = \frac{2 \int_0^{D/2} \rho \cdot C \cdot r \cdot \frac{\partial T_r^n}{\partial t} dr}{D} \quad (14)$$

$$h^n = \frac{2 \int_0^{D/2} \rho \cdot C \cdot r \cdot \frac{\partial T_r^n}{\partial t} dr}{D(T_\infty - T_R)} \quad (15)$$

where  $r$  is the radial coordinate;  $\Delta r$  the mesh spacing; and  $\alpha_i$  the thermal diffusivity.  $\eta$  and  $\eta'$  are very small numbers for the hyperbolic term.

It is noteworthy, that Eq. 14 is an integral expression of heat capacitance of the probe, which implies that the surface heat flux change equals to the internal heat capacitance change. Eq. 14 becomes identical to Eq. 10 if the cooling rate within the probe is uniform at any give time (the key assumption of the lumped capacitance model). The algorithms implemented in WinProbe have the capability of incorporating temperature dependent material properties.

### Experimental Procedure.

Stainless Steel 304 cylindrical probes of 1" diameter and 2" long (see figure 1) were used to measure the cooling curves. They were quenched in helium gas at a temperature of 28 °C and also in oil at 28, 30, 33 and 36 °C. Thermocouples were inserted in the center of each sample. A specially prepared testing apparatus was used to control the temperature.

The thermocouples were connected to a computer to carry out the data adquisition process, with a known frequency. These curves were then kept in numerical files which were afterwards used to feed INC-PHATRAN and WinProbe Code.

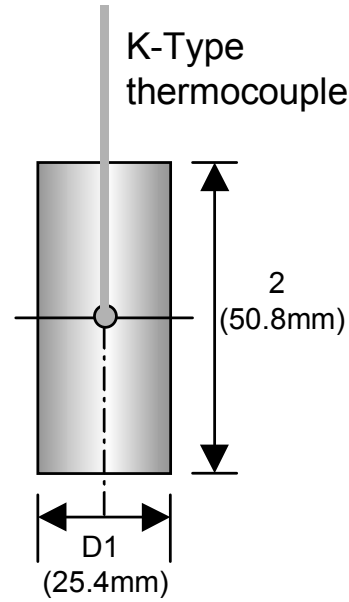


Figure 1. Schematic of 1" diameter 2" long stainless steel probe.

Figures 2 and 3 shows the measured cooling curves for both quenchants respectively.

### Modeling

INC-PHATRAN as well WinProbe were used to calculate the temperature dependent heat transfer coefficient corresponding to the 8 cooling curves showed in figures 2 and 3. Values of the thermal conductivity and the specific heat as depending of temperature, and of the density, are indicated in table 1.

Temperature dependent Thermal conductivity		Temperature dependent Specific Heat		Density
Temperature [°C]	Conductivity [w/m <sup>2</sup> K]	Temperature [°C]	Specific heat [J/kg.K]	[kg/m <sup>3</sup> ]
100.	16.3	38.	527.	7650.
204.	17.1	93.	549.	
427.	21.1	204.	567.	
500.	21.5	316.	586.	
649.	24.7	371.	601.	

Table 1: Thermophysical constant of the material considered in the modeling.

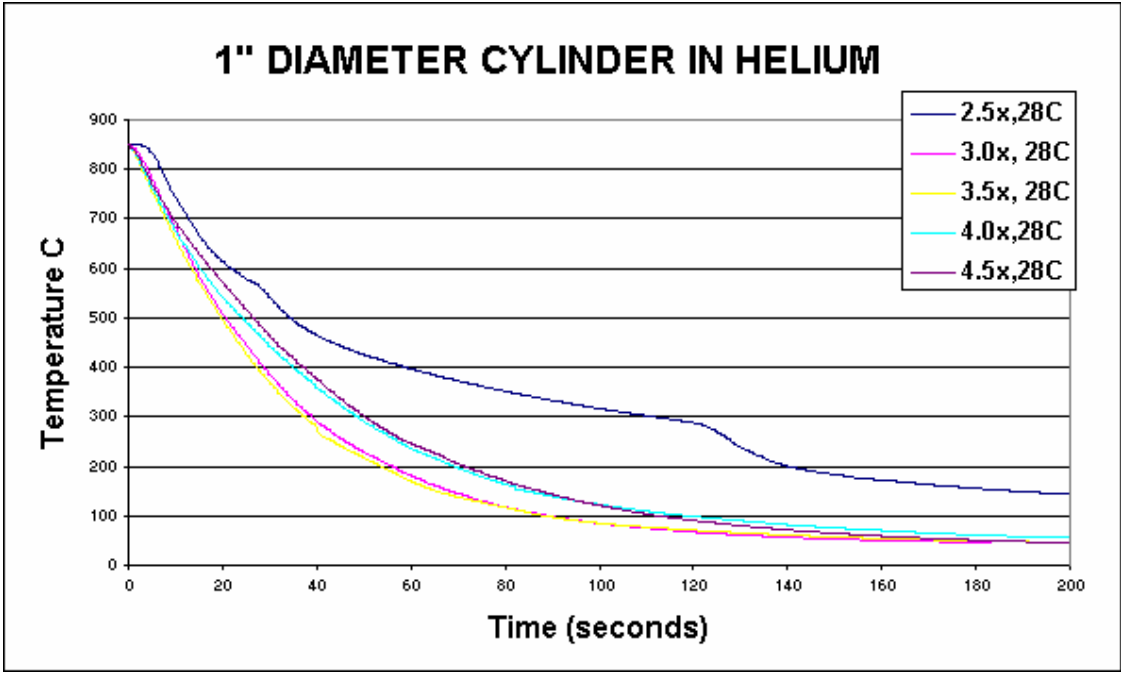


Figure 2. Cooling curves measured for 1" diameter probes of stainless steel 304 in helium.

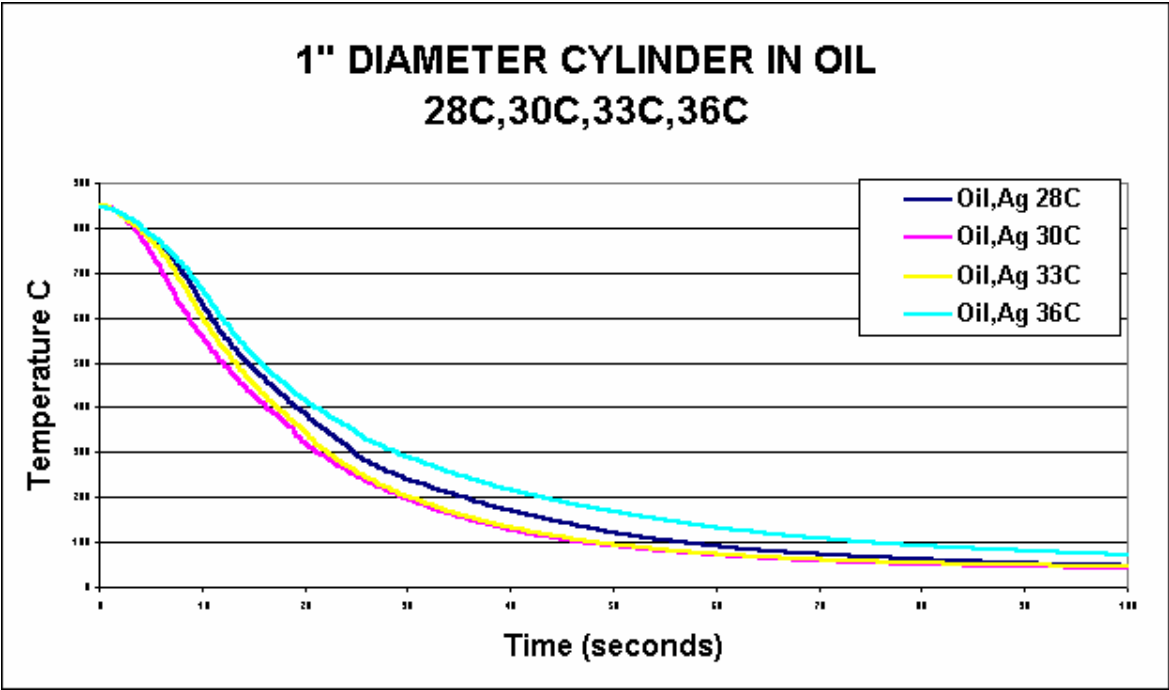


Figure 3. Cooling curves measured for 1" diameter probes of stainless steel 304 in oil at different temperatures.

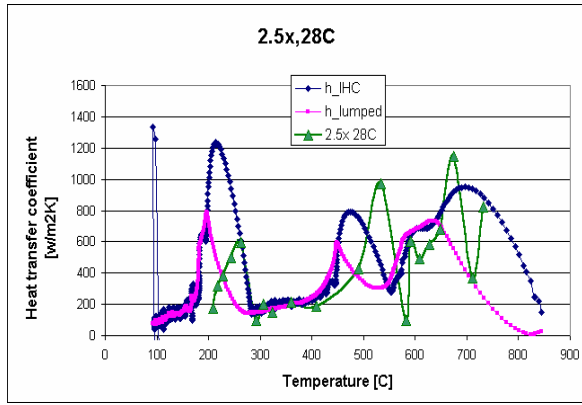


Figure 4: Comparisons of heat transfer coefficients calculated by INC-PHATRAN and WinProbe for 2.5x probes quenched in helium.

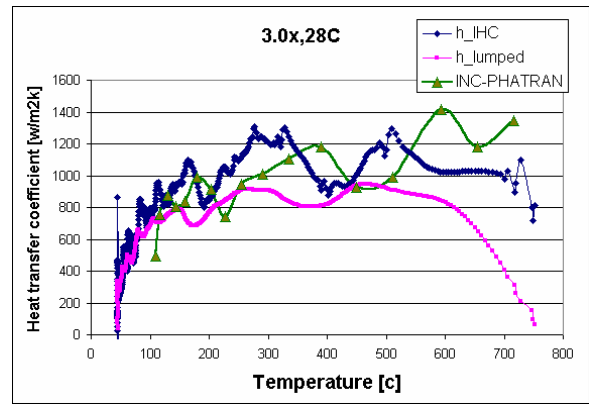


Figure 5: Comparisons of heat transfer coefficients calculated by INC-PHATRAN and WinProbe for 3.0x probes quenched in helium.

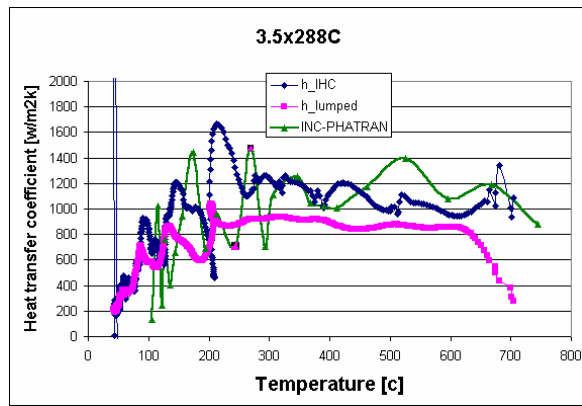


Figure 6: Comparisons of heat transfer coefficients calculated by INC-PHATRAN and WinProbe for 3.5x probes quenched in helium.

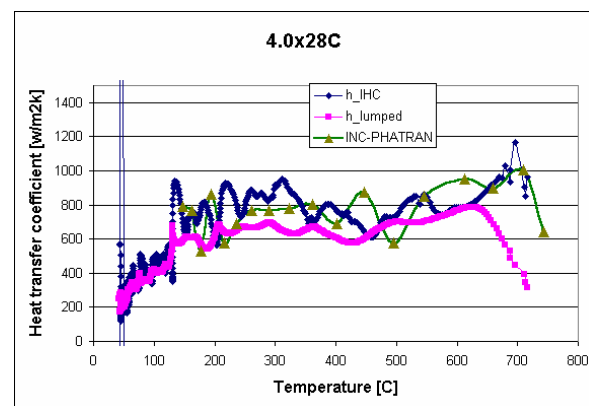


Figure 7: Comparisons of heat transfer coefficients calculated by INC-PHATRAN and WinProbe for 4.0x probes quenched in helium.

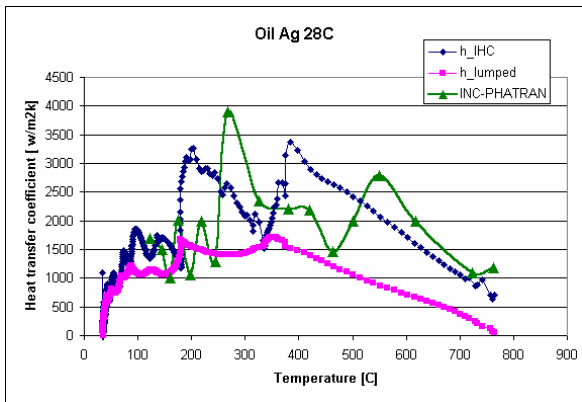


Figure 8: Comparisons of heat transfer coefficients calculated by INC-PHATRAN and WinProbe for probes quenched in oil at 28°C.

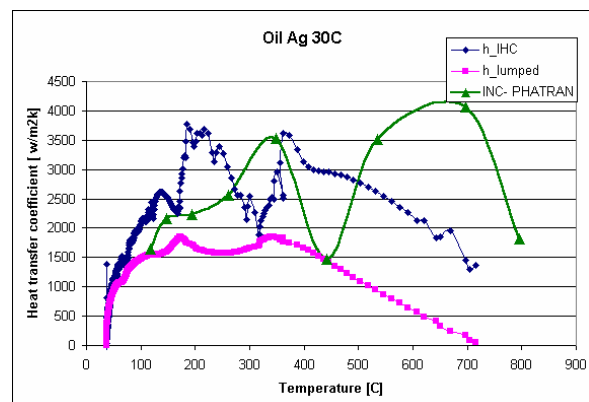


Figure 9: Comparisons of heat transfer coefficients calculated by INC-PHATRAN and WinProbe for probes quenched in oil at 30°C.

The heat transfer coefficient obtained by solving the Inverse Heat Conduction Problem (IHCP) by the WinProbe Code as well as by INC-PHATRAN code, and also using the Lumped Heat Capacitance Model of WinProbe, are compared in figures 4 to 11 separately for each cooling curve.

Curves of the figures show that results of INC-PHATRAN follows the results of the IHCP solved by WinProbe in a better way that the results of the Lumped Heat Capacitance Model.

#### Acknowledgements.

The authors thank the support given by Universidad de Buenos Aires, Argentina, through the Grant UBACYT TI035 (1998-2000).

#### References

1. X. Chen, L. Meekisho, M Becker and G.E. Totten, "A Numerical Validation of Lumped Capacitance Analysis for Deriving Heat Transfer Coefficient Using Quenching Probe", Proceedings of the 17<sup>th</sup> ASM-HTS Conference, Indianapolis, IN, September 15-18, 1997, ASM International, 1997, p. 355-361.
2. J.V. Beck, B. Blackwell and C.R.ST. Clair Jr., "Inverse Heat Conduction, Ill-posed Problems", John Wiley & Sons, New York, 1985.
3. G. Sánchez Sarmiento y C. Barragán, "INC-PHATRAN: A computer model for the simulation of heat-treating processes, User manual", SOFT-ING Consultores, Abril de 1997.
4. G. Sánchez Sarmiento, C. Barragán y J. Vega: "Predicting hardness distribution after heat treating processes of steels by finite element simulation combined with the SAE Standard J406". *Milam et al, Eds: HEAT TREATING - Proceedings of the 17th Heat Treat EXPO & Technical Conference*, ASM - Heat Treating Society, Indianapolis, USA, 15 al 18 de septiembre de 1997, pp 347-354.
5. G. Sánchez Sarmiento, A. Gastón y J. Vega: "Inverse heat conduction coupled with phase transformation problems in heat treating process". *E. Oñate and S.R. Idelsohn, Eds.: COMPUTATIONAL MECHANICS - New Trends and Applications*. CIMNE, Barcelona, España, 1998. CD-Book. Part VI, Section 1, Paper 16.
6. G. Sánchez Sarmiento, M.A. Morelli y J. Vega: "Improvements to the SAE J406 Hardenability Predictor". *R. Colás et al, Eds.: Proceedings of the 1st International Automotive Heat Treating Conference*, ASM International, Puerto Vallarta, México, 13 al 15 de julio de 1998, pp 401-414.
7. G. Sánchez Sarmiento, J. Vega, M.A. Morelli, J.C. Cuyás, A.I. Ledesma y M.J.A. Solari: "Predicting hardness of stainless steels in tempering cycles with variable temperature ". *Proceedings of the 19th ASM Heat Treat Expo & Technical Conference*, Cincinnati, OH, Nov. 1-4, 1999.
8. G. Sánchez Sarmiento y J. Vega: "Calculation of the hardness space distribution in the as quenched condition of a medium hardening tool steel". *1<sup>st</sup> International Conference on Thermal Process Modeling and Computer Simulation*, Shanghai Jiao Tong University, Shanghai, China, 28 al 30 de marzo de 2000.
9. X. Chen, L. Meekisho and G.E. Totten, "Computer-Aided Analysis of the Quenching Probe Test", Proceedings of the 18<sup>th</sup> ASM-HTS Conference, Chicago, IL, October 12-15, 1998, ASM International, 1998, p. 545-551.
10. X. Chen, L. Meekisho, G.E. Totten, Cooling Curve Analysis using 1" x 2" Stainless Steel Probe, Proceedings of the 19<sup>th</sup> ASM-HTS Conference, Cincinnati, Ohio, November 1-4, 1999, ASM International, 1999.

The main peaks of  $h(T)$  appears for temperatures higher by INC-PHATRAN than by WinProbe, in a systematic way.

The effects of noise presented in the cooling curves appears as the main cause of discrepancies between the IHCP solved by both codes. In a next stage, a new comparative study of the different algorithms will be performed after smoothing the cooling curves data.